AMERICAN SOCIETY FOR MICROBIOLOGY | Applied and Environmental Microbiology®

ENVIRONMENTAL MICROBIOLOGY

Accumulation and Dissolution of Magnetite Crystals in a Magnetically Responsive Ciliate

Caroline L. Monteil,[a] Nicolas Menguy,[b] Sandra Prévéral,[a] Alan Warren,[c] David Pignol,[a] Christopher T. Lefèvre[a]

[a]CNRS/CEA/Aix-Marseille Université, UMR7265 Biosciences and Biotechnologies Institute of Aix-Marseille, Saint-Paul-lés-Durance, France

[b]Sorbonne Université, UMR CNRS 7590, Muséum National d'Histoire Naturelle, IRD, Institut de Minéralogie, de Physique des Matériaux et de Cosmochimie, IMPMC, Paris, France

[c]Department of Life Sciences, Natural History Museum, London, United Kingdom

ABSTRACT Magnetotactic bacteria (MTB) represent a group of microorganisms that are widespread in aquatic habitats and thrive at oxic-anoxic interfaces. They are able to scavenge high concentrations of iron thanks to the biomineralization of magnetic crystals in their unique organelles, the so-called magnetosome chains. Although their biodiversity has been intensively studied, their ecology and impact on iron cycling remain largely unexplored. Predation by protozoa was suggested as one of the ecological processes that could be involved in the release of iron back into the ecosystem. Magnetic protozoa were previously observed in aquatic environments, but their diversity and the fate of particulate iron during grazing are poorly documented. In this study, we report the morphological and molecular characterizations of a magnetically responsive MTB-grazing protozoan able to ingest high quantities of MTB. This protozoan is tentatively identified as *Uronema marinum*, a ciliate known to be a predator of bacteria. Using light and electron microscopy, we investigated in detail the vacuoles in which the lysis of phagocytized prokaryotes occurs. We carried out high-resolution observations of aligned magnetosome chains and ongoing dissolution of crystals. Particulate iron in the ciliate represented approximately 0.01% of its total volume. We show the ubiquity of this interaction in other types of environments and describe different grazing strategies. These data contribute to the mounting evidence that the interactions between MTB and protozoa might play a significant role in iron turnover in microaerophilic habitats.

IMPORTANCE Identifying participants of each biogeochemical cycle is a prerequisite to our understanding of ecosystem functioning. Magnetotactic bacteria (MTB) participate in iron cycling by concentrating large amounts of biomineralized iron minerals in their cells, which impacts their chemical environment at, or below, the oxic-anoxic transition zone in aquatic habitats. It was shown that some protozoa inhabiting this niche could become magnetic by the ingestion of magnetic crystals biomineralized by grazed MTB. In this study, we show that magnetic MTB grazers are commonly observed in marine and freshwater sediments and can sometimes accumulate very large amounts of particulate iron. We describe here different phagocytosis strategies, determined using magnetic particles from MTB as tracers after their ingestion by the protozoa. This study paves the way for potential scientific or medical applications using MTB grazers as magnetosome hyperaccumulators.

KEYWORDS biomineralization, grazing, iron cycling, magnetite, magnetotactic bacteria, protozoa

Received 3 January 2018 **Accepted** 5 February 2018

Accepted manuscript posted online 9 February 2018

Citation Monteil CL, Menguy N, Prévéral S, Warren A, Pignol D, Lefèvre CT. 2018. Accumulation and dissolution of magnetite crystals in a magnetically responsive ciliate. Appl Environ Microbiol 84:e02865-17. https://doi.org/10.1128/AEM.02865-17.

Editor Robert M. Kelly, North Carolina State University

Address correspondence to Christopher T. Lefèvre, christopher.lefevre@cea.fr.

Iron is a micronutrient essential to the structure and function of several metalloproteins involved in a wide range of biochemical processes (oxygen transport, electron transfer, or redox reactions) that are directly or indirectly linked in many metabolic processes such as photosynthesis, diazotrophy, or respiration in anaerobic or aerobic environments (1, 2). Because iron is tightly coupled to other major nutrients, its cycling is a critical component of the global ecosystem functioning (3). The bioavailability of iron depends on its solubility and concentration (3). In well-oxygenated environments such as oceans, iron is mainly found in the +3 oxidation state, which is the most highly insoluble iron species that generally precipitates into diverse particulate forms such as oxides and carbonates. In less oxygenated environments, such as surface water sediments, iron is more reduced and soluble in a +2 oxidation state (4). Once dissolved, the majority of iron(III) or iron(II) is kept bioavailable to eukaryotes and prokaryotes through complexion with organic ligands (5). Identifying the main drivers of iron transformation, mobilization, and redistribution is important to understand and influence ecosystem functioning.

Under all natural conditions, microorganisms play a significant role in the transformations of iron, by the catalysis of iron reduction or oxidation, mineral dissolution, precipitation, or mineralization (6–8). A group of microorganisms called magnetotactic bacteria (MTB) has the singular ability to turn dissolved iron into particulates through biologically controlled mineralization under microaerobic or anaerobic conditions (9, 10). MTB biomineralize intracellular ferrimagnetic crystals into vesicles formed from the invagination of the periplasmic membrane (11, 12). Several of these singular structures, called magnetosomes, form one or several chains giving a magnetic moment parallel to the motility axis of the cell. Thanks to the coordination of the cell magnetic polarity, flagellum rotation, and chemoaerotaxis, the magnetotaxis function allows MTB to align and swim along magnetic field lines (9). Magnetosomes can be of different morphologies depending on the phylogenetic position and physiology of the bacterium, but one species generally biomineralizes only one type of particle (10). MTB are commonly found in aquatic habitats at the oxic-anoxic transition zone (OATZ), where they find optimum redox conditions for growth. While their biodiversity is well characterized, their function in this singular niche and their role in biogeochemical cycles have been poorly studied. Because of their ability to store approximately 100- to 1,000-fold higher iron concentrations than that of other microorganisms (13) and their significant contribution to the total microbial biomass (14, 15), it has been assumed that MTB contribute significantly to the biogeochemical cycle of iron with the potential to generate $>10^8$ kg of magnetite on a global scale per year (13). The release of biomineralized iron back to the microbial community depends on its dissolution once bacteria die (16, 17). In the absence of chelators and/or favorable pH, temperature, and light exposure, chemical dissolution of iron oxides is expected to be relatively modest (18). Acidic solutions exposed to light and containing some organic metal chelators favor *in vitro* chemical dissolution. For example, magnetite dissolution was observed at pH 4.5 in 0.1 M $NaClO_4$ at 25°C, but equilibrium was reached after only 20 days (19). Due to a lack of experimental evidence, it is difficult to determine the extent to which local natural environmental conditions are suitable for iron mineral dissolution and over what time range.

Biological processes and catalysts are known to speed up several chemical reactions and matter/energy turnover. Protozoan predation is an example of a biological process that is known to regulate bacterial biomass, productivity, and community structure (20). For iron turnover specifically, it has been shown that colloidal iron digestion by protozoa could generate iron in a form that is bioavailable for other organisms, including phytoplankton (21). Diverse protozoa, including flagellates, biflagellates, dinoflagellates, and ciliates containing intracellular magnetosome-like particles, have been reported from environmental samples (22 and references therein). The first evidence was given by Torres de Araujo and colleagues (23) who observed the magnetic response of a protozoan isolated from Fortaleza in Brazil containing numerous bullet-shaped magnetosome chains. Despite the lack of further evidence and

detailed ultrastructure characterization, it was speculated that this protozoan was biomineralizing the magnetosomes and performing magnetotaxis like that in MTB (22, 23). Indeed, since the arrangement of magnetosomes appeared to be precisely structured in the eukaryotic cells, it was assumed that this organization could not occur after grazing what would have to be significant numbers of MTB. Later, other magnetically responsive eukaryotes were observed in samples collected in Salt Pond, a semianoxic eutrophic marine basin in Woods Hole (MA, USA) (14, 24). Transmission electron microscopic observations showed that the protozoan cells contained particles with morphologies and dimensions identical to the those of the magnetosomes produced by MTB (24), suggesting an accumulation within the protozoa after the consumption and digestion of MTB. Grazing behavior was observed for some of these protozoa at the same time they became magnetically responsive after magnetosome ingestion. However, neither the fates of the magnetosomes in the protozoa nor the identities of the protozoa were further addressed in this study. Later, *in vitro* assays showed that the ciliate *Euplotes vannus* was able to dissolve greigite particles after ingestion of the multicellular magnetotactic bacterium "*Candidatus* Magnetoglobus multicellularis" (25), thus providing supplementary information on the trophic links with MTB. This was reported to occur in structures similar to protozoan food vacuoles, which are usually acidic, suggesting grazing to be the mechanism involved in mineral dissolution within the protozoan cell. Although useful, this laboratory experiment still requires validation using natural communities and other magnetic minerals such as magnetite.

Here, we present new data to shed light on the trophic interaction between MTB and their natural grazers. By using various approaches, including microscopy and molecular techniques, we report a population of magnetic protozoa able to graze MTB. We assess the ultrastructure of food vacuoles within the protozoan cells in which ingested magnetite magnetosomes are stored and fully degraded. We further discuss the implications such an interaction might have on the iron cycle and how this protozoon might have evolved and diversified to deal with iron toxicity and predation. We also propose some applications that could potentially be developed using eukaryotic vesicles magnetized by MTB.

RESULTS

Magnetically responsive organisms in samples from the Calanque of Méjean. All samples collected at the Calanque of Méjean, Marseille, France, contained $\sim 10^3$ cells/ml free-living MTB. These MTB were maintained in the samples for several months without significant variation in abundance or morphotypes. The shapes of the MTB cells and the shapes and organization of their magnetosomes, were similar to those of MTB commonly observed in marine environments, such as those already described from the Mediterranean Sea (26) (Fig. 1). At least eight different morphotypes of MTB were observed, likely representing eight different species. The small magnetotactic cocci biomineralizing two chains of elongated prismatic particles was the most abundant morphotype observed using both light and electron microscopy (Fig. 1A; see also Movie S1 in the supplemental material). Some magnetotactic cocci were quite large with an average diameter of 3 μm and biomineralizing a bundle of few cuboctahedral magnetosome chains (Fig. 1B). Cocci biomineralizing one chain of cuboctahedral magnetosomes were probably related to "*Candidatus* Magnetococcus massalia" (27), a similar magnetotactic bacterium isolated from the Pointe Rouge Marina (28) located near the Calanque of Méjean (Fig. 1C). Sequencing of the 16S rRNA gene of magnetically purified cells allowed the identification of five different operational taxonomic units (OTUs) that belong to the *Magnetococcaceae* family with 90 to 93% identity with *Magnetococcus marinus* strain MC-1 (29) and 93 to 99% identity with uncultured magnetotactic cocci (GenBank accession numbers KY569289 to KY569293). One 16S rRNA gene sequence obtained after magnetic purification had a 97% identity to the magnetotactic multicellular prokaryote (MMP) "*Ca*. Magnetoglobus multicellularis" (30) (accession number KY569294). Multicellular-like organisms were also observed by microscopy in the samples collected in the Calanque of Méjean (Fig. 1D). Their motility

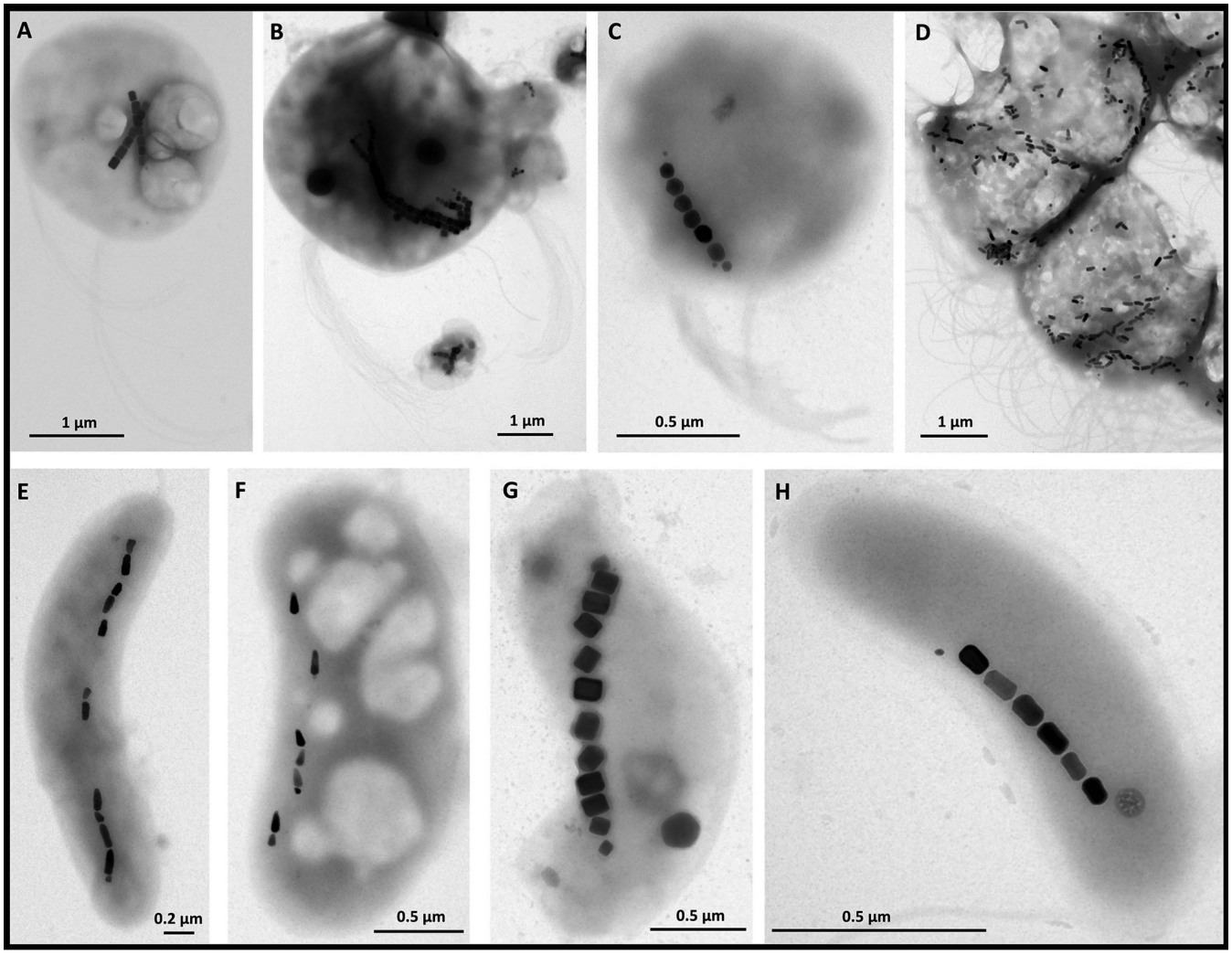

FIG 1 Transmission electron micrographs of magnetotactic bacteria isolated from the same sampling bottle collected from the Mediterranean Sea at the Calanque of Méjean near Marseille, France. At least 8 morphotypes were observed, including magnetotactic cocci of a different size that biomineralize one, two, or a cluster of chains of octahedral or elongated prismatic magnetosomes (A to C), a magnetotactic multicellular prokaryote that biomineralizes bullet-shaped magnetosomes (D), curved rods that biomineralize bullet-shaped magnetosomes (E and F), and spirilla or vibrios that biomineralize elongated prismatic magnetosomes (G and H). Note that only magnetite-type magnetosomes were observed. No MTB with magnetosomes resembling greigite were observed in this sample.

and ultrastructure were consistent with those of "*Ca*. Magnetoglobus multicellularis," although their bullet-shaped crystals are more likely to be made of magnetite (31), which differ from those of "*Ca*. Magnetoglobus multicellularis," which is known to produce greigite only. Different types of rods, vibrios, and spirilla biomineralizing cuboctahedral elongated prismatic or bullet-shaped magnetosomes were also observed to a lesser extent among the different MTB in samples collected from Calanque of Méjean (Fig. 1E to H).

One year after sampling, in addition to these morphologically diverse MTB, larger cells were also observed at the edge of a hanging drop harvested from the same samples from the Calanque of Méjean after 3 h of magnetic concentration (Fig. 2). Although the concentration of these large magnetic cells was much lower than that of MTB, it was sufficiently high in one sampling bottle to enable further characterization and identification. The dimensions of these organisms as well as their organelle-like structures (e.g., cilia) observed under the light microscope indicated that they were unicellular eukaryotes rather than prokaryotes (Fig. 2D). They were observed either stuck at the edge of the hanging drop where MTB were magnetically attracted (north

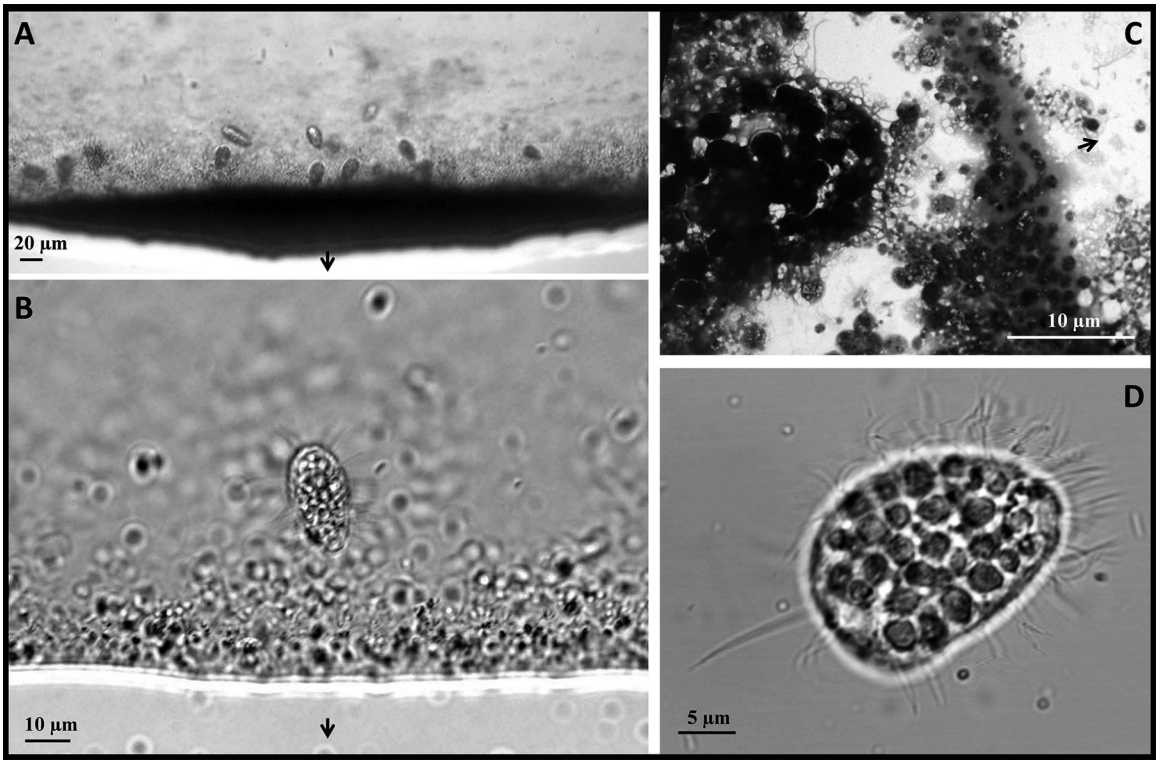

FIG 2 Light, confocal, and transmission electron microscopy of magnetically concentrated bacteria and protozoa. (A and B) Differential interference contrast microscopy images of the edge of a drop where magnetically responsive cells aggregate due to the presence of a magnet (in panel A, the dark precipitate is mostly composed of MTB with the coccoid cells being the most abundant). (C) TEM image of the edge of a drop (right side of the panel) where magnetically responsive cells aggregate due to the presence of a magnet. A magnetic protozoan can be seen on the left side of the panel. (D) Confocal microscopy image of a magnetic protozoan showing the numerous cilia surrounding the cell body as well as the presence of an elongated caudal cilium. In panels A to C, black arrows indicate the north direction of the artificial magnetic field generated close to the edge of the drop.

seeking) or moving along the edge of the drop. Occasionally, some eukaryotic cells were seen disturbing the MTB aggregated at the edge of the drop, using the cilia that cover their entire body (Fig. 2B and D). Such behavior could be considered part of the process of predation, and the eukaryotic cells were consequently shown to be a bacterivorous scuticociliate that graze on MTB (Movie S1).

At first glance, these protozoa seemed to have the same magnetic behavior as the MTB, that is, they migrate along magnetic field lines and respond to a reversal of the magnetic field by rotating 180° and continuing to swim in the same direction relative to the direction of the magnetic field. Evidence for a permanent magnetic dipole moment was also obtained by observing that nonswimming cells in suspension reoriented in response to a reversal of the local magnetic field. This effect is also typical of nonmotile (e.g., dead) MTB in suspension. On the basis of the sizes of these magnetic eukaryotic cells and their fast response to the inversion of a magnetic field, it is likely that they contained a significant amount of magnetic particles.

Identification of the magnetically responsive protozoan. Morphological features observed under confocal microscopy indicate that the magnetic eukaryote cells are scuticociliates. The body shape is elongated with a rounded posterior and a pointed anterior end and has an average length of 22.3 ± 1.5 μm and an average width of 14.3 ± 2.2 μm *in vivo* (Fig. 2D). Although it was difficult to observe the thickness of these organisms, they appear to be slightly dorsoventrally flattened approximately 2:1, with a thickness estimated at 5 to 10 μm on the basis of light microscopic observations. It has a prolonged caudal cilium, approximately 20 μm in length (Fig. 2D). Other somatic cilia are mostly approximately 10 μm long. Locomotion is highly characteristic when observed under the light microscope without an artificial magnetic field, often

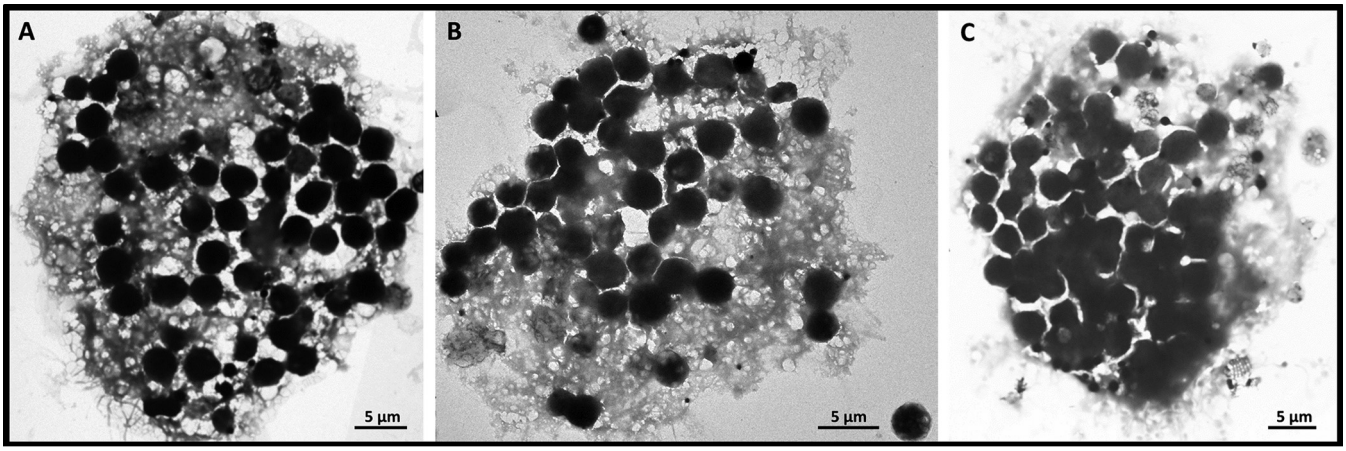

FIG 3 TEM bright-field images of magnetic protozoa disaggregated on a copper carbon-coated grid showing the presence of up to 50 vacuoles/cell.

stationary with all cilia stiffly spread, and then crawling with a rather smooth, sometimes helical, motion. The cytoplasm is colorless and packed with various numbers of vacuoles that are usually dark in color (Fig. 2D; see also Movies S2, S3, and S4). An average of 32 dark vacuoles per cell was counted, but some larger cells could contain up to 50 vacuoles (Fig. 3). More elaborate techniques are required for a detailed characterization of the ciliate morphology, including silver staining, which is beyond the scope of this paper.

The entire sequence of the 18S rRNA gene of the magnetic ciliates was obtained from magnetically concentrated and purified cells used for transmission electron microscopy (TEM) observations. The sequences of seven clones were identical to each other. The 18S rRNA gene sequence of the magnetic ciliate, designated clone Mj1 (GenBank accession number KY569295) showed 99.9% and 99.8% identities with that of *Parauronema virginianum* (AY392128) and *Uronema marinum* (GQ465466), respectively. A phylogenetic analysis based on the 18S rRNA gene confirmed its affiliation to the scuticociliate family Uronematidae in the order Philasterida (Fig. 4). The interspecific distance was smaller than 2%, indicating that members of the *Entodiscus*, *Parauronema*, and/or *Uronema* clade were probably misidentified and that a taxonomic reassessment is required (32). Since *Uronema marinum* was the first described genus and species of this clade (e.g., see reference 33), we use the name *U. marinum* in the following to describe the ciliate-grazing MTB from the Calanque of Méjean. Thus, on the basis of all morphological and molecular criteria, it is likely that clone Mj1 belongs to the species *U. marinum*.

Origin of the magnetic response of *Uronema marinum* Mj1. Scanning TEM-X-ray energy-dispersive spectroscopy (STEM-XEDS) elemental mapping indicated the presence of iron in the vacuoles of the magnetic ciliate *U. marinum* Mj1 (Fig. 5). These vacuoles also contained sulfur- and phosphorus-rich granules. Interestingly, the iron was not homogeneously distributed in the vacuoles but rather localized in chains that appear to be parallel one to another. This chain organization resembles that usually observed in MTB. Globules rich in S and P (in general, polyphosphates) are also common features observed in MTB (10).

The food vacuoles have an average diameter of 2.9 $\pm$ 0.4 μm. Their thickness may be quite problematic for conventional bright-field TEM observations at high magnification, since they are too dense for the electron beam to penetrate, so they appear very dark, making it difficult to observe their contents. However, either by adjusting the contrast of the images (Fig. 6A to D) or by using the STEM-high-angle annular dark field (HAADF) imaging mode (Fig. 6E to G), the content of the vacuole contents could be observed. Magnetosome-like particles were visualized in these vacuoles. Their origin was most likely from MTB grazed by the ciliate. Indeed, *U. marinum* is well known to be

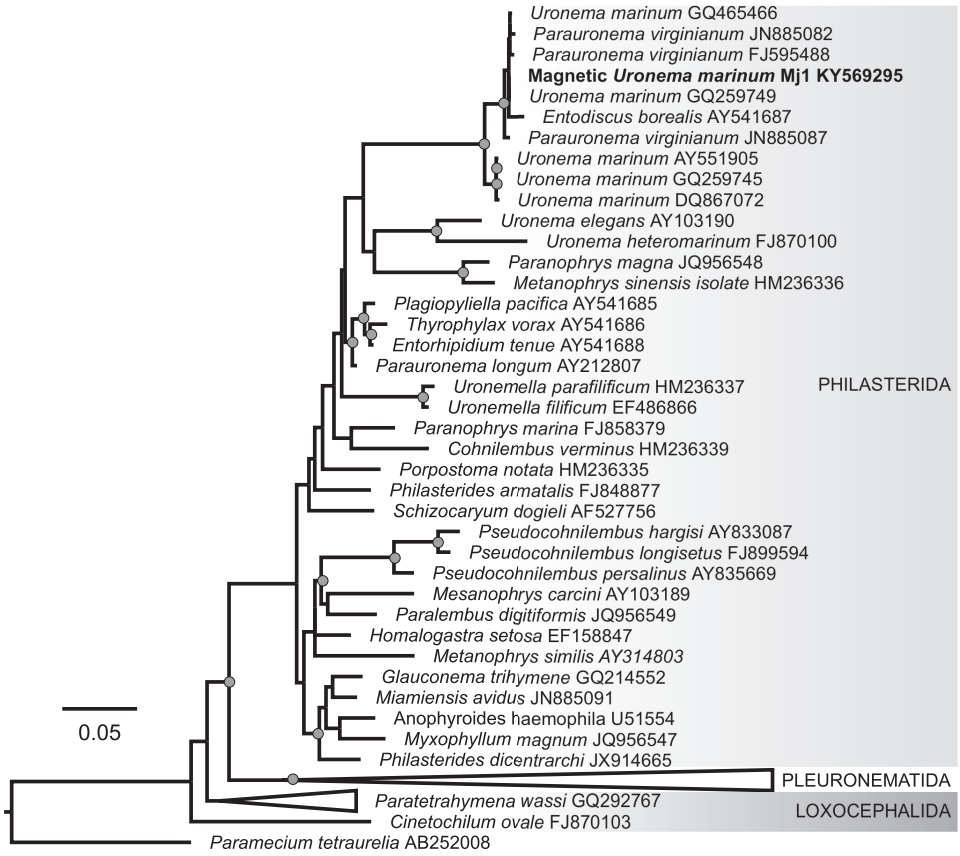

FIG 4 Maximum likelihood (ML) tree based on the 18S rRNA gene sequences of 55 ciliates showing the phylogenetic position of the magnetic ciliate *Uronema marinum* strain Mj1 within the subclass Scuticociliatia. The tree was inferred by estimating a GTRGAMMAI model to describe nucleotide evolution with RAxML 8.2.6 (68) and rooted with *Paramecium tetraurelia* strain 51. GenBank accession numbers are given next to strain names. The tree was drawn to scale, and branch lengths represent the number of base substitutions per site. A total of 599 bootstrap replicates automatically determined by the MRE-based bootstopping criterion were conducted under the rapid bootstrapping algorithm to test robustness of the nodes, among which 100 were sampled to generate proportional support values. Nodes annotated with gray circles are supported by bootstrap values higher than 70%.

a bacterivore that feeds voraciously on bacteria associated with decaying organic matter (34). Moreover, most organisms that biomineralize magnetosomes are able to produce only one type of particle, whereas the magnetosomes found in the food vacuoles of *U. marinum* Mj1 comprise a variety of different morphologies (e.g., cuboctahedral, elongate prismatic, or bullet shaped) (Fig. 6H). Interestingly, magnetosomes were intact and still aligned in chains, with some showing evidence of ongoing degradation. Moreover, the majority of magnetosome chains within the same vacuole were aligned in parallel to each other. This suggests that an actin-like filament persists in the vacuoles even if most of the magnetotactic cells were already lysed in the vacuoles. The magnetosomes and the sulfur and polyphosphate globules are probably the most recalcitrant prokaryotic structures to be digested in the ciliate and are the bacterial components that remain the longest in the vacuoles before degradation.

The cell membrane of *U. marinum* MJ1 appears to be quite fragile. Indeed, when adsorbed on the carbon film of the TEM grid, most of the cells disaggregate (Fig. 3 and 5), and the dark vacuoles spread. Thus, from the TEM pictures, it is difficult to know if all the magnetosome chains from the different vacuoles were in the same orientation when the cell was still alive. However, when the vacuoles from the same ciliate cell remained closely adjacent on the TEM grid (Fig. 6A), the majority of magnetosome chains from the different vacuoles appears to be aligned in the same direction, i.e.,

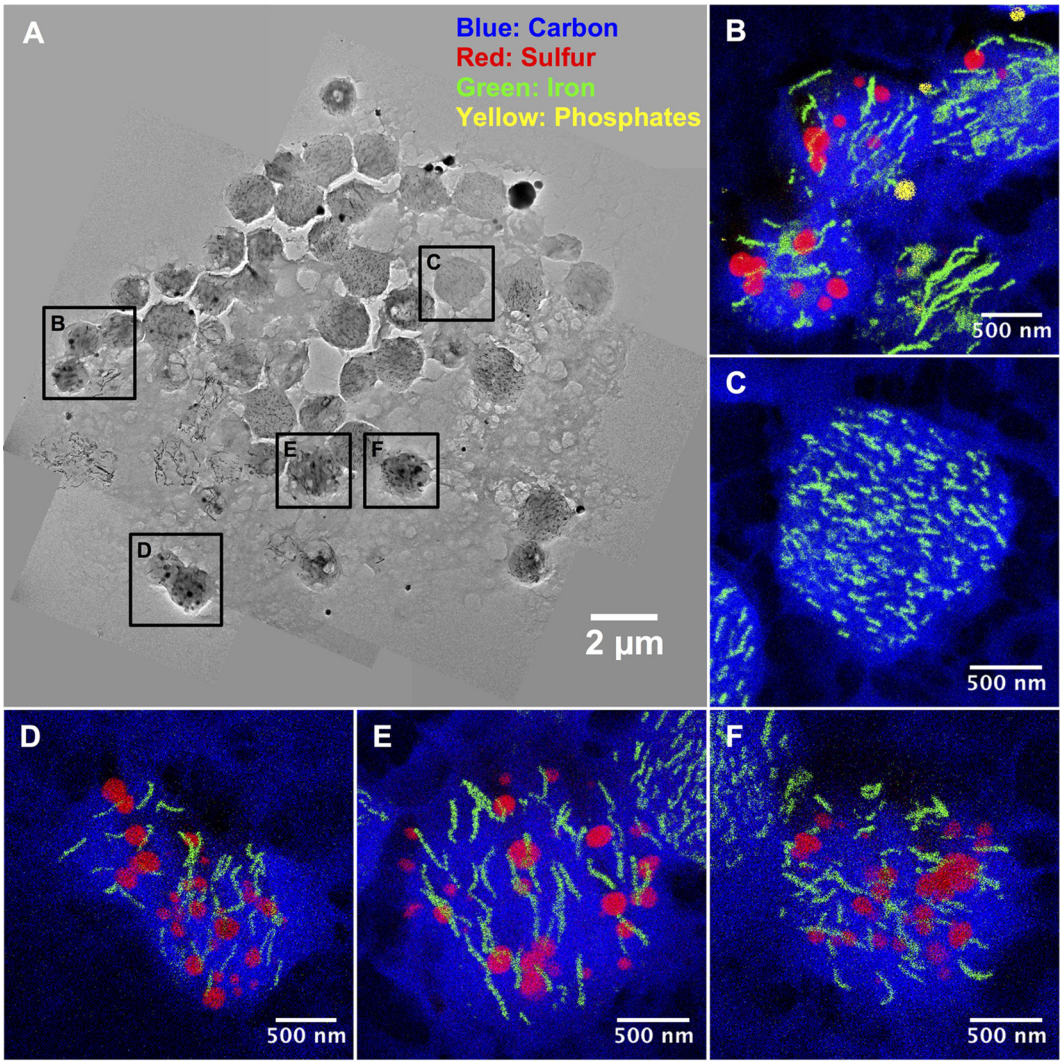

FIG 5 Assembled TEM bright-field images of a magnetic protozoan adsorbed on a carbon-coated grid (A) and STEM-XEDS elemental maps of carbon, sulfur, iron and phosphorus, showing a large amount of iron in the vacuoles as well as the presence of sulfur- and phosphate-rich granules (B to F).

along the long axis of the cell. This would explain the fact that *U. marinum* Mj1 is very responsive to the inversion of the magnetic field.

On average, 446 $\pm$ 94 mature magnetosomes of different morphologies per vacuole were present. On the basis of the average number of vacuoles per protozoan (i.e., 32), there were approximately 14,272 magnetosomes on average in a single ciliate cell, reaching a maximum of 22,300. If we suppose that each MTB has an average of 10 magnetosomes, at least 1.4×10^3 MTB on average must have been grazed by each individual ciliate. Further investigations would be necessary to determine the ingestion rate over time. Extrapolating the shape of the ciliate cells to an ellipsoid and that of the vacuoles and magnetosomes to spheres of 2.5 μm and 50 nm in diameter, respectively, we estimate that the vacuoles and magnetosomes represent approximately 6% and 0.01%, respectively, of the volume of the ciliate cell.

Magnetosome dissolution by the magnetic protozoa. High-resolution TEM (HR-TEM) and energy-dispersive X-ray spectroscopy analyses were performed in food vacuoles that had burst. Indeed, due to the adsorption of the ciliate cells onto the carbon film of the TEM grid, some vacuoles had lost their integrity and released their contents, facilitating the observation of the particles present (see Fig. 8A). Note that the

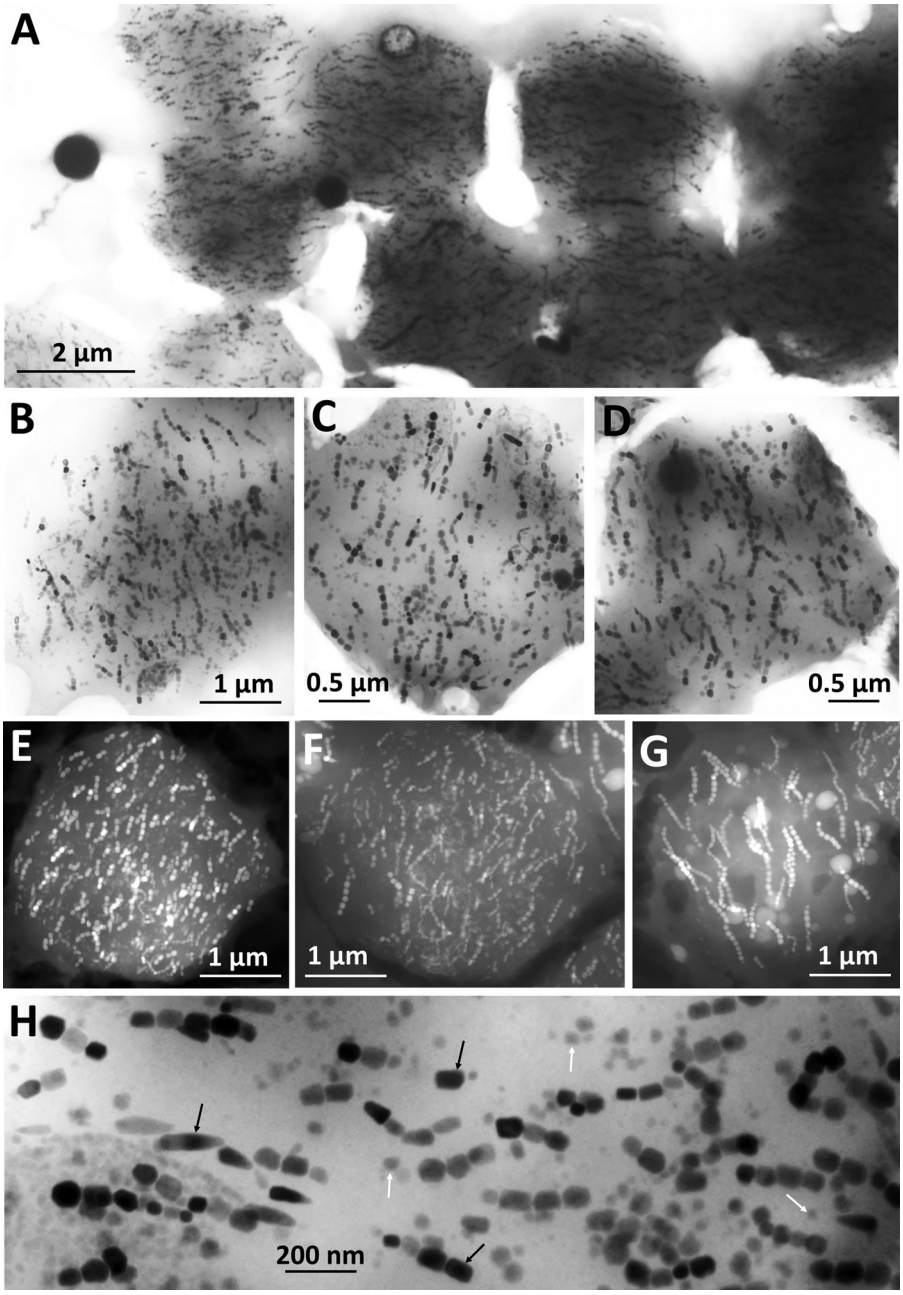

FIG 6 Conventional TEM bright-field (A to D and H) and STEM-HAADF (E to G) images of the dark vacuoles found in *Uronema marinum* Mj1 showing the presence of numerous morphologically diverse linearly aligned magnetosome-like particles. Arrows in panel H point to examples of integral (black arrows) and partially dissolved (white arrows) magnetosomes.

magnetosome alignment in individual chains was conserved in disrupted vacuoles while the parallel alignment of chains was not.

Although most magnetosome chains and magnetosomes appeared very similar to those observed in MTB (Fig. 1), some magnetosomes had suffered partial dissolution (Fig. 6H). Interestingly, the dissolution process seems to depend on the morphology type of magnetosomes (Fig. 7). Indeed, cuboctahedral particles appear to be preferentially dissolved from specific faces (possibly [110] ones) (Fig. 7A, B, and C), while the dissolution of bullet-shaped particles was always observed at the flattened end and then digested toward the pointed end (Fig. 7D).

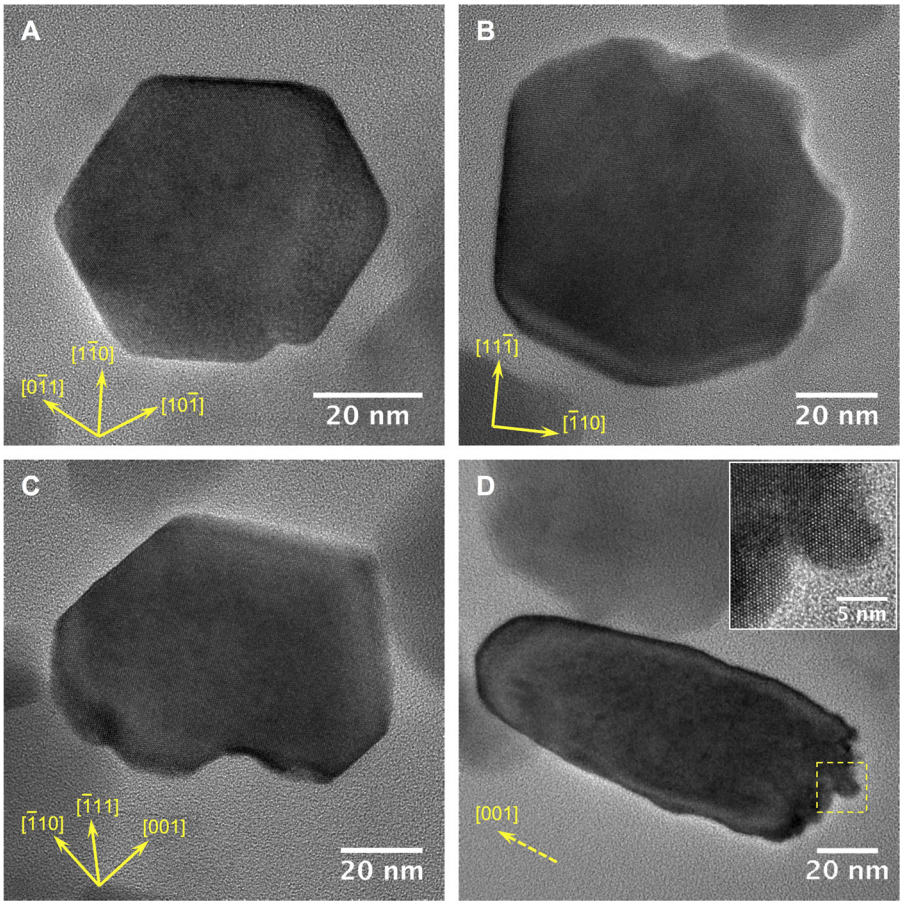

FIG 7 High-resolution transmission electron micrographs of cuboctahedral (A to C) and bullet-shaped (D) magnetite magnetosomes in a food vacuole of *U. marinum* Mj1 showing structural defects due to partial dissolution. For each crystal, main crystallographic directions are indicated.

In the vicinity of the magnetosome chains, some mineral phases that were less electron dense than the magnetosomes were observed (Fig. 8). An elemental analysis indicates that these amorphous structures are mainly composed of Fe, O, P, Mg, and Ca and represent the remains of dissolved magnetosomes (Fig. 8A and B), while selected area (electron) diffraction (SAED) patterns indicate that these particles are consistent with iron phosphate (Fig. 8D). While iron and part of the oxygen originate from magnetite (Fe_3O_4) of dissolved magnetosomes, the phosphorus, magnesium, calcium, and oxygen most probably originate from polyphosphate granules of ingested magnetotactic bacteria (Fig. 5).

Evidence for the ubiquity of magnetically responsive MTB grazers. Given the successful observation of a magnetically responsive ciliate in a sample from the Calanque of Méjean, it was hypothesized that increasing the magnetic concentration time might reveal a greater diversity of such MTB grazers in other environments. To test this hypothesis, we collected sediment and water samples from a freshwater lake (Lake Pavin, Auvergne, France), another site in the Mediterranean Sea (Pointe Rouge marina, Marseille, France), and other locations at the Calanque of Méjean and screened these for magnetically responsive protozoa by applying the same protocol. After at least 3 h of magnetic concentration, we could observe in most samples diverse protozoan assemblages with different cell morphologies and sizes that stored magnetosomes differently (examples are shown in Fig. S1 to S3). Not all protozoa had the ability to sequester the magnetosomes in vacuoles as observed for *Uronema marinum* Mj1. For instance, an unidentified freshwater protozoan seemed to keep the magnetosomes in chains homogeneously distributed in the cell body (Fig. S1A and B), similar to certain

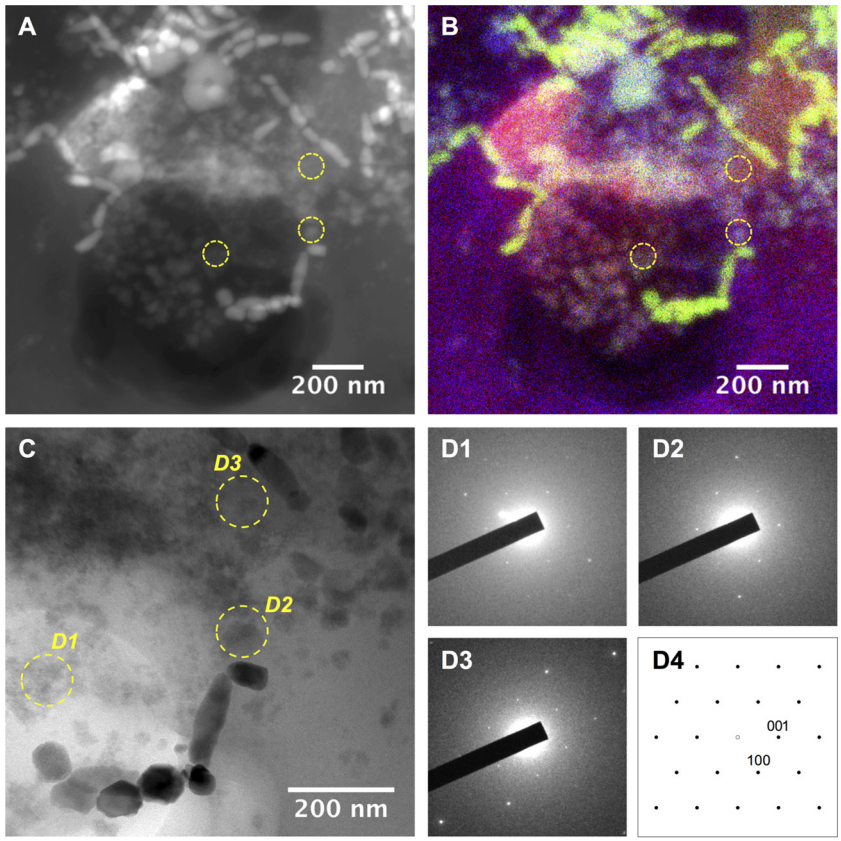

FIG 8 Analysis of less electron dense particles observed in the food vacuoles of *Uronema marinum* Mj1. STEM-HAADF (A) and corresponding STEM-XEDS elemental mapping (B). Magnetite magnetosomes appear with a bright contrast in panel A and as green areas in panel B, whereas iron phosphate phases are related to gray particles in panel A and bright particles in panel B. (C) TEM bright-field image revealing magnetosomes surrounded by less dense electron particles. (D, 1 to 3) SAED patterns related to areas labeled in panel C. These SAED patterns are consistent with a [010] zone axis diffraction pattern of $FePO_4{\cdot}H_2O$ phase (D4; SAED calculated using crystallographic data from reference 69).

unidentified weakly magnetic biflagellates collected at the Calanque of Méjean having few magnetosome particles (Fig. S2).

In samples from the Pointe Rouge marina, light microscope and TEM observations indicated the presence of two magnetic ciliates (Fig. 9A; see also Fig. S3A and B). One was morphologically similar to *U. marinum* Mj1 and could be related to the *Uronema* genus (Fig. S3C). Interestingly, in this ciliate, magnetosome chains were not always stored in vacuoles and were not aligned with each other (Fig. S3C and D). However, MTB grazing was supported by the fact that the ciliate contained three types of particles, elongate prismatic, cuboctahedral, and bullet shaped, which corresponded to the magnetosome diversity that could be observed in free-living MTB communities of this sample (Fig. S3D to F). The second magnetic ciliate from the Pointe Rouge marina had a very different shape and would be most likely a pleurostomatid (class Litostomatea) on the basis of its morphology *in vivo*: the cell body is slightly contractile, with the posterior and anterior ends bluntly pointed. Interestingly, the diversity of magnetosomes ingested supported the idea the grazing behavior of this magnetic protozoan specifically was more selective. Indeed, only elongated prismatic magnetosomes were observed in the cytoplasm of this protozoan, while MTB communities formed very diverse types of magnetite crystals (Fig. 9B to E; see also Fig. S3E and F). Moreover, the magnetosomes seemed to have accumulated in the anterior pointed end of the cell and formed long chains in this specific location (Fig. 9B to E). The MTB that produce elongated prismatic magnetosomes are cocci with a diameter of 1 to 2 μm; it is possible that this type of protozoan can only graze bacteria with such size. It is also

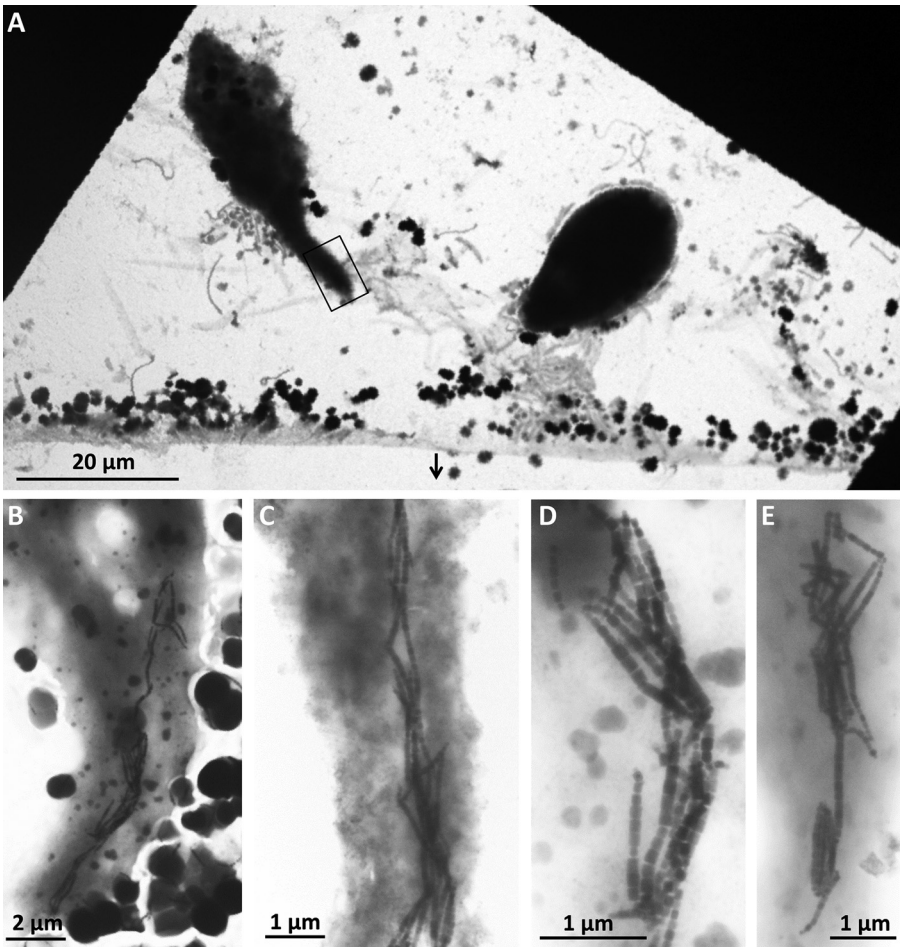

FIG 9 (A) Transmission electron microscopic (TEM) images of the edge of the drop of a magnetically concentrated sample from Pointe Rouge marina, Marseille, showing two types of MTB-grazing protozoa. The sizes of these organisms are typical of eukaryotic cells with a length of 38 μm and a width of 11.4 μm for the cell on the left side of the panel and a length of 22.4 μm and a width of 12.2 μm for the cell on the right side of the panel. (B to E) TEM images of the anterior pointed end of the protozoan morphologically related to the pleurostomatid that grazes only one type of MTB, i.e., magnetotactic cocci with elongated prismatic particles.

possible that these magnetotactic cocci have a different chemical composition that makes them more attractive to this protozoan. Interestingly, pleurostomatids are known to be carnivorous, feeding on flagellates and other ciliates (35). If this organism is a pleurostomatid, then it has likely acquired the MTB by ingesting eukaryotic prey (flagellates or ciliates) containing MTB.

DISCUSSION

Since the discovery of MTB, few studies have addressed the fate of iron once biomineralized in magnetosomes in environmental conditions. Yet, determining the processes involved in iron turnover is critical to understand ecosystem functioning. Grazing has been proposed as one of the processes that could recycle particulate iron back to the communities through dissolution (20). In this study, we brought new insights into MTB grazing by reporting natural populations of magnetically responsive ciliates that internalize significant amounts of magnetosomes in specific intracellular compartments, within which we found evidence of their dissolution. We showed that diverse protozoa can graze MTB in both freshwater and marine environments and that this trophic interaction might be common in aquatic habitats with a redox gradient. One sample collected from the Mediterranean Sea at the Calanque of Méjean near Marseille, France, had a sufficient concentration of an MTB-grazing ciliate, nominally

identified as *Uronema marinum*, to enable the characterization of magnetosome digestion within its food vacuoles.

Uronema marinum is a cosmopolitan marine ciliate. Representative strains of this species are facultative parasites and one of the main causative agents of outbreaks of scuticociliatosis in aquaculture fish. The cultivation of *U. marinum* is possible using bacteria (e.g., *Vibrio* sp.) as a food source (36) or using more complex growth media (37). Using a transformed fluorescent *Vibrio* strain, it was shown that *U. marinum*, along with other ciliates, is able to ingest up to 10^5 bacteria · ciliate^{-1} · h^{-1} (38). Ingestion rates of the marine ciliates are higher with surface-associated prey than with bacteria in suspension. Thus, it is not surprising that MTB can be predated by bacterivorous ciliates, especially at the oxic-anoxic transition zone where bacteria are attached to the sediment or on the glass walls of sampling bottles during magnetic enrichment. MTB have the advantage of being traceable after ingestion by a protozoan predator due to the magnetosomes that remain intact for a long period after ingestion before their gradual dissolution. Here, *in situ* observation of ongoing dissolution was possible because sufficient intact magnetosomes were present to enable the magnetic concentration of MTB grazers. The high number of magnetosomes, MTB cells, and food vacuoles in a single ciliate cell (i.e., 446 $\pm$ 94 magnetosomes per vacuole and up to 50 vacuoles per cell), suggests that MTB grazers such as *U. marinum* may play an important role in iron cycling. Our observations suggest that total magnetosome dissolution is achieved during the life cycle of the ciliate, but it was very difficult to observe this directly, since cells should become magnetically unresponsive as the magnetosomes dissolve. Quantification of such grazers coupled to their cultivation would be required to estimate the impact of this trophic interaction on the iron cycle and to determine the selection pressure exerted by predation on MTB populations and diversification.

In this study, various morphotypes of magnetosomes were observed in the food vacuoles of magnetic *U. marinum* Mj1, suggesting that the ciliate did not select the type of MTB grazed. However, in another sample at the Pointe Rouge marina, we found evidence for another protozoan species selecting one type of MTB. This suggests that protozoa could be more or less specialized while grazing MTB and nonmagnetotactic bacteria. This opens questions regarding the evolutionary mechanisms that led to the evolution of each partner; did they coevolve to become dependent on each other or is MTB grazing simply opportunistic, provoked by the fact both organisms share the same niche? Some strains of *U. marinum* have been described as microaerobic ciliates with the potential to be facultative anaerobes (39). Since *Uronema* is often present in the same biotopes as MTB (i.e., the oxic-anoxic interface in aquatic habitats), it is likely that it has adapted and developed strategies to deal with the high concentration of iron that accumulates in their cells while grazing MTB. It is also possible that MTB grazers have evolved to specifically ingest MTB in order to become magnetic.

MTB grazers could benefit from their passive orientation with the magnetic field lines in order to locate regions of low oxygen concentration, as demonstrated for MTB (40). Indeed, some protozoa have been described to use specific mechanisms such as aerotaxis to find their optimal oxygen concentration (41). The fact that the magnetosome chains within the food vacuoles of *U. marinum* Mj1 remain intact (Fig. 6 and 9) could be a specific adaptation to have the best magnetic dipole moment to optimize the magnetic response. Indeed, in MTB, the total magnetic dipole moment of the cell is the algebraic sum of the moments of the individual crystals in the chain (42). Although, the magnetosome chains present in the food vacuoles of *U. marinum* Mj1 were smaller than those biomineralized in MTB, it is likely that neither the MamK filament nor the magnetosome membrane were totally lysed. Indeed, in some cultivated magnetotactic species, both the MamK filament and the magnetosome membrane are necessary to keep the magnetosomes aligned in the chain (43). It is interesting to question whether *U. marinum* Mj1 has developed a specific mechanism to keep the magnetosomes aligned in the food vacuoles or if the magnetic field keeps the magnetosome chains aligned in the same direction. The fact that the magnetic cells of *U. marinum* Mj1 change direction when the polarity of the magnetic field is switched

indicates that the magnetosome chains are fixed in position within the food vacuoles. Moreover, the food vacuoles do not seem to rotate within the cells when the local magnetic field is rotated. Thus, the magnetosome chains in the ciliate stay aligned within ingested MTB cells until these cells are digested or a specific mechanism has been developed by the ciliate to keep the magnetosome chains aligned in the same direction once MTB have been digested.

Importantly, the internalization of MTB and their magnetosome chains appears to vary depending on the protozoa that graze them. Here, we evidenced at least three strategies observed in three morphologically diverse protozoa: (i) the internalization of magnetosomes that remain aligned in food vacuoles by *U. marinum* Mj1, (ii) the accumulation of one type of selected elongated prismatic magnetosomes in the anterior pointed end of an unidentified ciliate, and (iii) the apparently random storage of magnetosome chains in the cell of a biflagellate. The latter strategy was already described in a dinoflagellate isolated from a seasonally, chemically stratified coastal salt pond in Massachusetts, USA (24). The extruded magnetic inclusions, previously described for a biflagellate (24), could potentially represent another strategy where the magnetosomes are stored in vacuoles resembling those observed in *U. marinum* Mj1 and then be expelled from the protozoan cell body, avoiding the need to dissolve the magnetic particles. Previous studies showed the mechanism by which ciliates eject undigested material in their food vacuoles via the cytoproct (44). In this study, such excretions outside magnetic *U. marinum* Mj1 cells were never observed. The internalization of hundreds of magnetosomes in single vacuoles may prevent the toxic effects of high iron content, such as in MTB, with the magnetosome membrane surrounding the magnetic particles (12, 45), but questions remain on how protozoa deal with the iron toxicity as the magnetosomes progressively dissolve. This question is even more complex knowing that some protozoa did not internalize MTB in vacuoles. Since we could observe magnetic particles with different degrees of degradation until amorphous phases, we can deduce that magnetosomes are totally dissolved within the food vacuoles of *U. marinum* Mj1. Interestingly, this process appeared to be directed toward specific regions of the crystal depending on the morphology of the particle. This observation is particularly intriguing, since it suggests that the ferromagnetic crystal shape has an impact on dissolution kinetics. It is possible that each type of magnetosome coexists with different ligands, promoting various levels of protonation, complexation, or reduction mechanisms involved in dissolution, as previously suggested (46). The remaining questions concern the mechanisms involved in the release of the dissolved iron and how the cells deal with iron toxicity. Ciliates are known to defecate undigested material via their cytoproct (44). Thus, after the magnetosomes are degraded and lysed, it is likely that the bioavailable colloidal iron is expelled from the cell via the cytoproct. However, further experimentation is needed to verify this.

Naturally magnetically responsive protozoa have previously been described in the water column of the seasonally stratified Salt Pond, MA, USA (14, 24). In addition, a cultivated strain of *Euplotes vannus* has been shown to ingest the multicellular magnetotactic prokaryote and greigite-producing "*Ca*. Magnetoglobus multicellularis" (25) and to partially dissolve magnetic particles. Here, we revealed that the diversity of protozoa able to become magnetic by grazing MTB is greater than previously realized, in freshwater sediments and in marine sediments. Thus, there is mounting evidence that magnetic protozoa have been overlooked, although they may be widespread in chemically stratified aquatic ecosystems. The systematic magnetic concentration of samples over a period of several hours might enable the characterization and isolation of new types of MTB grazers that contribute to the recycling of iron present in the magnetosomes of MTB.

Magnetite-producing MTB and their magnetic inclusions have been used in a variety of scientific, commercial, and environmental applications (47–50). Moreover, MTB are inspiring the field of synthetic biology with the transformation of nonmagnetic organisms into magnetic ones using biogenic magnetization approaches (51, 52). With the discovery of MTB-grazing protozoa, we can envision a synthetic magnetization with

the cocultivation of MTB with heterotrophic protozoa. This could be very useful for the sequestration of magnetosomes and their concentration into individual eukaryotic cells and might significantly improve some medical applications (e.g., drug delivery) that have been so far developed using cultured MTB (53–55). Heterotrophic bacteriovorus *U. marinum* and related species have been cultivated for years and are available in culture collections (36, 37). Thus, such improvements can be relatively simple to test. Ciliates and other unicellular eukaryotes have developed unique motility apparatus from a simple flagellum to more complex rows of cilia (56). Making such organisms magnetic will enable the ease of manipulation in microfluidics chambers and facilitate the characterization of their movement and motility apparatus, such as has been achieved with magnetically controlled magnetotactic cells (57, 58). Finally, determining the mechanisms of intracellular biodegradation of iron oxide nanoparticles is of high interest in public health, particularly in regenerative medicine, where the fate of nanoparticles present within engineered tissue is a critical issue (59). The use of MTB grazers as models could provide critical information on the degradation of magnetite particles that resemble iron oxide particles generally used in medical applications.

MATERIALS AND METHODS

Sample collection, isolation, and observation of magnetic and magnetotactic organisms. Samples were collected in September 2015 by freediving in the Mediterranean Sea, at the Calanque of Méjean near Marseille, France (43.330875°N, 5.218548°E). One-liter plastic bottles were filled to approximately 0.2 to 0.3 of their maximum volume with sediment, and then filled to their capacity with water that overlaid the sediment. Air bubbles were excluded. Once in the laboratory, samples were stored under dim light at room temperature (~25°C). This confinement creates an oxygen gradient at equilibrium allowing the microbial communities to be maintained while selecting for some populations that are enriched. Magnetotactic populations were observed the day of their collection, and were checked 1 year later to see if any new magnetotactic organisms could have been enriched. For each observation, magnetotactic cells were magnetically concentrated by placing the south pole of a magnetic stirring bar next to sample bottles at the sediment-water interface for 3 h and then further purified using the capillary magnetic racetrack technique (60). The examination of concentrated magnetotactic cells was carried out using the hanging drop technique (61) under a Leica LMD6000 and a Zeiss Primo Star light microscope equipped with phase-contrast and differential interference contrast (DIC) optics. The local magnetic field used to determine magnetotaxis was reversed by rotating a stirring bar magnet 180° on the microscope stage.

Morphological characterization of magnetic protozoa. Morphological features of protozoa were determined with a confocal microscope. A z-stack of 18 to 59 images was captured at focal planes with a step distance of 0.4 μm using a Zeiss LSM780 confocal microscope equipped with a Plan-Apochromat 63×/1.40 oil DIC M27 objective.

Transmission electron microscopy (TEM) was used to give new insights into the ultrastructure of these organisms. The magnetic protozoan ultrastructure could partially be observed thanks to an improved technique to fix magnetic cells on a TEM carbon-coated grid. This technique consists of pipetting 2 μl of liquid from the edge of the hanging drop where magnetic cells aggregated and slowly depositing these cells onto the TEM grid to have one edge of this small drop in the middle of the grid. Then, the magnetic cells were magnetically attracted to this edge over a 10-min period. Once the drop started to dry, the grid was washed with filtered deionized water. This technique facilitates the observation and enables optimal adsorption of the magnetic cells onto the carbon film.

Electron micrographs were recorded with a Tecnai G2 BioTWIN transmission electron microscope (FEI Company) at a 100-kV acceleration voltage. High-resolution transmission microscopy (HRTEM), z-contrast imaging in the high-angle annular dark field (STEM-HAADF) mode, and X-ray energy-dispersive spectroscopy (XEDS) elemental mapping in the STEM-XEDS mode were carried out on a JEOL 2100F microscope. This machine, operating at 200 kV, is equipped with a Schottky emission gun, an ultrahigh-resolution pole piece, and an ultrathin window JEOL XEDS detector. HRTEM images were obtained with a Gatan US4000 charge-coupled-device (CCD) camera.

Magnetosomes present in protozoan cells were enumerated from TEM images using ImageJ software (1.48 v).

Cloning and sequencing of the 18S and 16S rRNA genes of magnetically purified cells. The 18S and 16S rRNA genes were used to identify magnetically concentrated MTB-grazing protozoa and free-living MTB, respectively. Genomic DNA was extracted using the NucleoSpin soil extraction kit (Macherey-Nagel). DNA was amplified using the Phusion hot start Flex DNA polymerase according to the manufacturer's recommendations. For eukaryotes, specific 18S rRNA gene primers EukA (5′-AACCTGGT TGATCCTGCCAGT-3′) and EukB (5′-TGATCCTTCTGCAGGTTCACCTAC-3′) (62) were used. For bacteria, the primers 27F (5′-AGAGTTTGATCMTGGCTCAG-3′) and 1492R (5′-TACGGHTACCTTGTTACGACTT-3′) (63) were used. Blunt-end fragments of 16S and 18S rRNA gene sequences were cloned using a Zero Blunt TOPO PCR Cloning kit with One Shot TOP10 chemically competent *Escherichia coli* cells. The inserts of resulting clones were digested using restriction enzymes to select operational taxonomic units (OTUs)

representative of the populations and were sent for sequencing and compared to the NCBI nucleotide database with the Basic Local Alignment Search Tool. For the eukaryote, this first step enabled its taxonomic assignment to the ciliate subclass Scuticociliatia (phylum Ciliophora, class Oligohymenophorea) pending further phylogenetic investigation.

Phylogenetics and identification of the purified ciliates. A phylogenetic tree was built to infer the evolutionary relationships between the magnetic ciliate and representative scuticociliate species. The contiguous 18S rRNA gene sequence of the ciliate was aligned with 54 selected and published sequences (64–66) using MUSCLE (67). The hymenostome *Paramecium tetraurelia* was selected as the outgroup. The alignment resulted in 1,788 bp, among which, position 717 was polymorphic once all ambiguous positions were removed. A maximum likelihood (ML) tree was built with RAxML 8.2.6 (68) under the GAMMAI model of rate heterogeneity using empirical nucleotide frequencies and the GTR nucleotide substitution model. A total of 599 bootstrap replicates automatically determined by the magnitude of relative error (MRE)-based bootstopping criterion were conducted under the rapid bootstrapping algorithm, among which 100 were sampled to generate proportional support values.

Accession number(s). The 16S rRNA gene sequences of MTB isolated from environmental samples were deposited in GenBank under accession numbers KY569289 to KY569294.

SUPPLEMENTAL MATERIAL

Supplemental material for this article may be found at https://doi.org/10.1128/AEM.02865-17.

SUPPLEMENTAL FILE 1, PDF file, 0.5 MB.
SUPPLEMENTAL FILE 2, AVI file, 7.3 MB.
SUPPLEMENTAL FILE 3, AVI file, 0.9 MB.
SUPPLEMENTAL FILE 4, AVI file, 0.8 MB.
SUPPLEMENTAL FILE 5, AVI file, 0.4 MB.

ACKNOWLEDGMENTS

C.L.M. and C.T.L. were funded by the French National Research Agency (ANR-16-TERC-0025-01). C.L.M., N.M., S.P., D.P., and C.T.L. acknowledge support within the framework of a DFG-ANR project (ANR-14-CE35-0018). Support for the microscopy equipment was provided by the HélioBiotec platform, funded by the European Union (European Regional Development Fund), the Région Provence Alpes Côte d'Azur, the French Ministry of Research, and the Commissariat à l'Energie Atomique et aux Energies Alternatives.

We thank Hélène Javot for help with optical microscopy.

REFERENCES

1. Lindley PF. 1996. Iron in biology: a structural viewpoint. Rep Prog Phys 59:867. https://doi.org/10.1088/0034-4885/59/7/002.
2. Liu J, Chakraborty S, Hosseinzadeh P, Yu Y, Tian S, Petrik I, Bhagi A, Lu Y. 2014. Metalloproteins containing cytochrome, iron–sulfur, or copper redox centers. Chem Rev 114:4366–4469. https://doi.org/10.1021/cr400479b.
3. Tagliabue A, Bowie AR, Boyd PW, Buck KN, Johnson KS, Saito MA. 2017. The integral role of iron in ocean biogeochemistry. Nature 543:51–59. https://doi.org/10.1038/nature21058.
4. Worsfold PJ, Lohan MC, Ussher SJ, Bowie AR. 2014. Determination of dissolved iron in seawater: a historical review. Mar Chem 166:25–35. https://doi.org/10.1016/j.marchem.2014.08.009.
5. Gledhill M, Buck KN. 2012. The organic complexation of iron in the marine environment: a review. Front Microbiol 3:69. https://doi.org/10.3389/fmicb.2012.00069.
6. Ghiorse WC. 1984. Biology of iron- and manganese-depositing bacteria. Annu Rev Microbiol 38:515–550. https://doi.org/10.1146/annurev.mi.38.100184.002503.
7. Tortell PD, Maldonado MT, Granger J, Price NM. 1999. Marine bacteria and biogeochemical cycling of iron in the oceans. FEMS Microbiol Ecol 29:1–11. https://doi.org/10.1111/j.1574-6941.1999.tb00593.x.
8. Kappler A, Straub KL. 2005. Geomicrobiological cycling of iron. Rev Mineral Geochem 59:85–108. https://doi.org/10.2138/rmg.2005.59.5.
9. Bazylinski DA, Frankel RB. 2004. Magnetosome formation in prokaryotes. Nat Rev Microbiol 2:217–230. https://doi.org/10.1038/nrmicro842.
10. Lefèvre CT, Bazylinski DA. 2013. Ecology, diversity, and evolution of magnetotactic bacteria. Microbiol Mol Biol Rev 77:497–526. https://doi.org/10.1128/MMBR.00021-13.
11. Blakemore R. 1975. Magnetotactic bacteria. Science 190:377–379. https://doi.org/10.1126/science.170679.
12. Gorby YA, Beveridge TJ, Blakemore RP. 1988. Characterization of the bacterial magnetosome membrane. J Bacteriol 170:834–841. https://doi.org/10.1128/jb.170.2.834-841.1988.
13. Lin W, Pan Y, Bazylinski DA. 2017. Diversity and ecology of and biomineralization by magnetotactic bacteria. Environ Microbiol Rep 9:345–356. https://doi.org/10.1111/1758-2229.12550.
14. Simmons SL, Edwards KJ. 2007. Geobiology of magnetotactic bacteria, p 77–102. *In* Schüler D (ed), Magnetoreception and magnetosomes in bacteria. Springer, Berlin, Germany.
15. Faivre D, Schüler D. 2008. Magnetotactic bacteria and magnetosomes. Chem Rev 108:4875–4898. https://doi.org/10.1021/cr078258w.
16. Vali H, Kirschvink J. 1989. Magnetofossil dissolution in a paleomagnetically unstable deep-sea sediment. Nature 339:203–206. https://doi.org/10.1038/339203a0.
17. Bazylinski DA, Moskowitz BM. 1997. Microbial biomineralization of magnetic iron minerals: microbiology, magnetism and environmental significance. Rev Mineral 35:181–223.
18. Cornell RM, Schwertmann U. 2003. Dissolution, p 297–344. The iron oxides. Wiley-VCH, Weinheim, Germany.
19. Sun Z-X, Su F-W, Forsling W, Samskog P-O. 1998. Surface characteristics of magnetite in aqueous suspension. J Colloid Interface Sci 197:151–159. https://doi.org/10.1006/jcis.1997.5239.
20. Sherr EB, Sherr BF. 2002. Significance of predation by protists in aquatic microbial food webs. Antonie Van Leeuwenhoek 81:293–308. https://doi.org/10.1023/A:1020591307260.
21. Barbeau K, Moffett JW, Caron DA, Croot PL, Erdner DL. 1996. Role of

protozoan grazing in relieving iron limitation of phytoplankton. Nature 380:61–64. https://doi.org/10.1038/380061a0.
22. Bazylinski DA, Lefèvre CT, Frankel RB. 2012. Magnetotactic protists at the oxic-anoxic transition zones of coastal aquatic environments, p 133–143. *In* Altenbach AV, Bernhard JM, Seckbach J (ed), Anoxia: evidence for eukaryote survival and paleontological strategies. Springer, Dordrecht, Netherlands.
23. Torres de Araujo FF, Pires MA, Frankel RB, Bicudo CEM. 1986. Magnetite and magnetotaxis in algae. Biophys J 50:375–378. https://doi.org/10.1016/S0006-3495(86)83471-3.
24. Bazylinski DA, Schlezinger DR, Howes BH, Frankel RB, Epstein SS. 2000. Occurrence and distribution of diverse populations of magnetic protists in a chemically stratified coastal salt pond. Chem Geol 169:319–328. https://doi.org/10.1016/S0009-2541(00)00211-4.
25. Martins JL, Silveira TS, Abreu F, Silva KT, da Silva-Neto ID, Lins U. 2007. Grazing protozoa and magnetosome dissolution in magnetotactic bacteria. Environ Microbiol 9:2775–2781. https://doi.org/10.1111/j.1462-2920.2007.01389.x.
26. Lefèvre CT, Bernadac A, Pradel N, Wu LF, Yu-Zhang K, Xiao T, Yonnet J-P, Lebouc A, Song T, Fukumori Y. 2007. Characterization of Mediterranean magnetotactic bacteria. J Ocean Univ China 6:355–359. https://doi.org/10.1007/s11802-007-0355-4.
27. Ji B, Zhang S-D, Zhang W-J, Rouy Z, Alberto F, Santini C-L, Mangenot S, Gagnot S, Philippe N, Pradel N, Zhang L, Tempel S, Li Y, Médigue C, Henrissat B, Coutinho PM, Barbe V, Talla E, Wu L-F. 2017. The chimeric nature of the genomes of marine magnetotactic coccoid-ovoid bacteria defines a novel group of *Proteobacteria*. Environ Microbiol 19:1103–1119. https://doi.org/10.1111/1462-2920.13637.
28. Lefèvre CT, Bernadac A, Yu-Zhang K, Pradel N, Wu L-F. 2009. Isolation and characterization of a magnetotactic bacterial culture from the Mediterranean Sea. Environ Microbiol 11:1646–1657. https://doi.org/10.1111/j.1462-2920.2009.01887.x.
29. Bazylinski DA, Williams TJ, Lefèvre CT, Berg RJ, Zhang CL, Bowser SS, Dean AJ, Beveridge TJ. 2013. *Magnetococcus marinus* gen. nov., sp. nov., a marine, magnetotactic bacterium that represents a novel lineage (*Magnetococcaceae* fam. nov.; Magnetococcales ord. nov.) at the base of the *Alphaproteobacteria*. Int J Syst Evol Microbiol 63:801–808. https://doi.org/10.1099/ijs.0.038927-0.
30. Abreu F, Martins JL, Silveira TS, Keim CN, de Barros HGPL, Filho FJG, Lins U. 2007. "*Candidatus* Magnetoglobus multicellularis," a multicellular, magnetotactic prokaryote from a hypersaline environment. Int J Syst Evol Microbiol 57:1318–1322. https://doi.org/10.1099/ijs.0.64857-0.
31. Kolinko S, Richter M, Glöckner F-O, Brachmann A, Schüler D. 2014. Single-cell genomics reveals potential for magnetite and greigite biomineralization in an uncultivated multicellular magnetotactic prokaryote. Environ Microbiol Rep 6:524–531. https://doi.org/10.1111/1758-2229.12198.
32. Hubert N, Hanner R. 2015. DNA barcoding, species delineation and taxonomy: a historical perspective. DNA barcodes 3:44–58. https://doi.org/10.1515/dna-2015-0006.
33. Kruger F, Wohlfarthbottermann K, Pfefferkorn G. 1952. Protistenstudien.3. Die Trichocysten von *Uronema marinum* Dujardin. Z Naturforsch B J Chem Sci 7:407–410.
34. Zubkov MV, Sleigh MA. 2000. Comparison of growth efficiencies of protozoa growing on bacteria deposited on surfaces and in suspension. J Eukaryot Microbiol 47:62–69. https://doi.org/10.1111/j.1550-7408.2000.tb00012.x.
35. Lynn DH. 2008. The ciliated protozoa: characterization, classification, and guide to the literature, 3rd ed. Springer, New York, NY.
36. Gast V. 1985. Bacteria as a food source for microzooplankton in the Schlei Fjord and Baltic Sea with special reference to ciliates. Mar Ecol Prog Ser 22:107–120. https://doi.org/10.3354/meps022107.
37. Zheng W, Gao F, Warren A. 2015. High-density cultivation of the marine ciliate *Uronema marinum* (Ciliophora, Oligohymenophorea) in axenic medium. Acta Protozool 54:325–330.
38. Tuorto SJ, Taghon GL. 2014. Rates of benthic bacterivory of marine ciliates as a function of prey concentration. J Exp Mar Biol Ecol 460:129–134. https://doi.org/10.1016/j.jembe.2014.06.014.
39. Bernard C, Fenchel T. 1996. Some microaerobic ciliates are facultative anaerobes. Eur J Protistol 32:293–297. https://doi.org/10.1016/S0932-4739(96)80051-4.
40. Frankel RB, Bazylinski DA, Johnson MS, Taylor BL. 1997. Magneto-aerotaxis in marine coccoid bacteria. Biophys J 73:994–1000. https://doi.org/10.1016/S0006-3495(97)78132-3.
41. Fenchel T, Finlay BJ. 1984. Geotaxis in the ciliated protozoon *Loxodes*. J Exp Biol 110:17–33.
42. Penninga I, Dewaard H, Moskowitz BM, Bazylinski DA, Frankel RB. 1995. Remanence measurements on individual magnetotactic bacteria using a pulsed magnetic-field. J Magn Magn Mater 149:279–286. https://doi.org/10.1016/0304-8853(95)00078-X.
43. Uebe R, Schüler D. 2016. Magnetosome biogenesis in magnetotactic bacteria. Nat Rev Microbiol 14:621–637. https://doi.org/10.1038/nrmicro.2016.99.
44. Allen R. 1974. Food vacuole membrane growth with microtubule-associated membrane-transport in *Paramecium*. J Cell Biol 63:904–922. https://doi.org/10.1083/jcb.63.3.904.
45. Andrews SC, Robinson AK, Rodriguez-Quinones F. 2003. Bacterial iron homeostasis. FEMS Microbiol Rev 27:215–237. https://doi.org/10.1016/S0168-6445(03)00055-X.
46. Banwart S, Davies S, Stumm W. 1989. The role of oxalate in accelerating the reductive dissolution of hematite (α-Fe_2O_3) by ascorbate. Colloids Surf 39:303–309. https://doi.org/10.1016/0166-6622(89)80281-1.
47. Lang C, Schüler D, Faivre D. 2007. Synthesis of magnetite nanoparticles for bio- and nanotechnology: genetic engineering and biomimetics of bacterial magnetosomes. Macromol Biosci 7:144–151. https://doi.org/10.1002/mabi.200600235.
48. Matsunaga T, Arakaki A. 2007. Molecular bioengineering of bacterial magnetic particles for biotechnological applications, p 227–254. *In* Schüler D (ed), Magnetoreception and magnetosomes in bacteria. Springer, Berlin, Germany.
49. Xie J, Chen K, Chen X. 2009. Production, modification and bio-applications of magnetic nanoparticles gestated by magnetotactic bacteria. Nano Res 2:261–278. https://doi.org/10.1007/s12274-009-9025-8.
50. Alphandéry E. 2014. Applications of magnetosomes synthesized by magnetotactic bacteria in medicine. Front Bioeng Biotechnol 2:5. https://doi.org/10.3389/fbioe.2014.00005.
51. Nishida K, Silver PA. 2012. Induction of biogenic magnetization and redox control by a component of the target of rapamycin complex 1 signaling pathway. PLoS Biol 10:e1001269. https://doi.org/10.1371/journal.pbio.1001269.
52. Kolinko I, Lohße A, Borg S, Raschdorf O, Jogler C, Tu Q, Pósfai M, Tompa E, Plitzko JM, Brachmann A, Wanner G, Müller R, Zhang Y, Schüler D. 2014. Biosynthesis of magnetic nanostructures in a foreign organism by transfer of bacterial magnetosome gene clusters. Nat Nanotechnol 9:193–197. https://doi.org/10.1038/nnano.2014.13.
53. Taherkhani S, Mohammadi M, Daoud J, Martel S, Tabrizian M. 2014. Covalent binding of nanoliposomes to the surface of magnetotactic bacteria for the synthesis of self-propelled therapeutic agents. ACS Nano 8:5049–5060. https://doi.org/10.1021/nn5011304.
54. Chen C, Chen L, Yi Y, Chen C, Wu L-F, Song T. 2016. Killing of *Staphylococcus aureus* via magnetic hyperthermia mediated by magnetotactic bacteria. Appl Environ Microbiol 82:2219–2226. https://doi.org/10.1128/AEM.04103-15.
55. Felfoul O, Mohammadi M, Taherkhani S, de Lanauze D, Zhong Xu Y, Loghin D, Essa S, Jancik S, Houle D, Lafleur M, Gaboury L, Tabrizian M, Kaou N, Atkin M, Vuong T, Batist G, Beauchemin N, Radzioch D, Martel S. 2016. Magneto-aerotactic bacteria deliver drug-containing nanoliposomes to tumour hypoxic regions. Nat Nanotechnol 11:941–947. https://doi.org/10.1038/nnano.2016.137.
56. Ginger ML, Portman N, McKean PG. 2008. Swimming with protists: perception, motility and flagellum assembly. Nat Rev Microbiol 6:838–850. https://doi.org/10.1038/nrmicro2009.
57. Murat D, Hérisse M, Espinosa L, Bossa A, Alberto F, Wu L-F. 2015. Opposite and coordinated rotation of amphitrichous flagella governs oriented swimming and reversals in a magnetotactic spirillum. J Bacteriol 197:3275–3282. https://doi.org/10.1128/JB.00172-15.
58. Pierce CJ, Mumper E, Brown EE, Brangham JT, Lower BH, Lower SK, Yang FY, Sooryakumar R. 2017. Tuning bacterial hydrodynamics with magnetic fields. Phys Rev E 95:062612. https://doi.org/10.1103/PhysRevE.95.062612.
59. Mazuel F, Espinosa A, Luciani N, Reffay M, Le Borgne R, Motte L, Desboeufs K, Michel A, Pellegrino T, Lalatonne Y, Wilhelm C. 2016. Massive intracellular biodegradation of iron oxide nanoparticles evidenced magnetically at single-endosome and tissue levels. ACS Nano 10:7627–7638. https://doi.org/10.1021/acsnano.6b02876.
60. Wolfe RS, Thauer RK, Pfennig N. 1987. A "capillary racetrack" method for isolation of magnetotactic bacteria. FEMS Microbiol Ecol 3:31–35. https://doi.org/10.1111/j.1574-6968.1987.tb02335.x.

61. Schüler D. 2002. The biomineralization of magnetosomes in *Magnetospirillum gryphiswaldense*. Int Microbiol 5:209–214. https://doi.org/10.1007/s10123-002-0086-8.
62. Medlin L, Elwood HJ, Stickel S, Sogin ML. 1988. The characterization of enzymatically amplified eukaryotic 16S-like rRNA-coding regions. Gene 71:491–499. https://doi.org/10.1016/0378-1119(88)90066-2.
63. Lane DJ. 1991. 16S/23S sequencing, p 115–175. *In* Stackebrandt E, Goodfellow M (ed), Nucleic acid techniques in bacterial systematics. John Wiley & Sons, New York, NY.
64. Pan H, Huang J, Hu X, Fan X, Al-Rasheid KAS, Song W. 2010. Morphology and SSU rRNA gene sequences of three marine ciliates from Yellow Sea, China, including one new species, *Uronema heteromarinum* nov spec. (Ciliophora, Scuticociliatida). Acta Protozool 49:45–59.
65. Pan X, Huang J, Fan X, Ma H, Al-Rasheid KAS, Miao M, Gao F. 2015. Morphology and phylogeny of four marine scuticociliates (Protista, Ciliophora), with descriptions of two new species: *Pleuronema elegans* spec. nov and *Uronema orientalis* spec nov. Acta Protozool 54:31–43.
66. Gao F, Warren A, Zhang Q, Gong J, Miao M, Sun P, Xu D, Huang J, Yi Z, Song W. 2016. The all-data-based evolutionary hypothesis of ciliated protists with a revised classification of the phylum Ciliophora (Eukaryota, Alveolata). Sci Rep 6:24874. https://doi.org/10.1038/srep24874.
67. Edgar RC. 2004. MUSCLE: multiple sequence alignment with high accuracy and high throughput. Nucleic Acids Res 32:1792–1797. https://doi.org/10.1093/nar/gkh340.
68. Stamatakis A. 2014. RAxML version 8: a tool for phylogenetic analysis and post-analysis of large phylogenies. Bioinformatics 30:1312–1313. https://doi.org/10.1093/bioinformatics/btu033.
69. Song Y, Zavalij PY, Suzuki M, Whittingham MS. 2002. New iron(III) phosphate phases: crystal structure and electrochemical and magnetic properties. Inorg Chem 41:5778–5786. https://doi.org/10.1021/ic025688q.